Drug Design, Development and Therapy

Dovepress
open access to scientific and medical research

Open Access Full Text Article

ORIGINAL RESEARCH

Sevoflurane Improves Ventricular Conduction by Exosomes Derived from Rat Cardiac Fibroblasts After Hypothermic Global Ischemia-Reperfusion Injury

Yanyan Ma[1,*], Ying Cao[2,*], Hong Gao[3], Rui Tong[1], Jing Yi[3], Zhongwei Zhang[1], Rui Chen[1], Zhijun Pan[1]

[1]School of Anesthesia, Guizhou Medical University, Guiyang, People's Republic of China; [2]Department of Anesthesiology, The Second People's Hospital of Guiyang, Guiyang, People's Republic of China; [3]Department of Anesthesiology, The Affiliated Hospital of Guizhou Medical University, Guiyang, People's Republic of China

*These authors contributed equally to this work

Correspondence: Hong Gao, Department of Anesthesiology, The Affiliated Hospital of Guizhou Medical University, No. 9 Beijing Road, Guiyang, People's Republic of China, Email 2169617@qq.com; anesth@qq.com

Purpose: This study investigated the effect of exosomes derived from sevoflurane-treated cardiac fibroblasts (Sev-CFs-Exo) on reperfusion arrhythmias (RA), ventricular conduction, and myocardial ischemia-reperfusion injury (MIRI).

Methods: Primary cardiac fibroblasts (CFs) were isolated from the hearts of neonatal rats and identified by morphology and immunofluorescence. Exosomes were isolated from CFs at passages 2–3 after they had been treated with 2.5% sevoflurane for an hour and cultivated for 24–48 hours. The control group was CFs that did not receive any treatment. The hypothermic global ischemia-reperfusion injury model was established using the Langendorff perfusion technique following injection with exosomes through the caudal vein. Multi-electrode array (MEA) mapping was used to investigate the changes in RA and ventricular conduction in isolated hearts. Western blots and immunofluorescence were used to examine the relative expression and location of connexin 43 (Cx43). In addition, the MIRI was evaluated with triphenyl tetrazolium chloride and Hematoxylin-Eosin staining.

Results: The primary CFs had a variety of morphologies, no spontaneous pulsation, and were vimentin-positive, which confirmed their successful isolation. Sev-CFs-Exo increased the heart rate (HR) at reperfusion for 15 minutes (T_2) and 30 minutes (T_3) and lowered the score and duration of RA and the time for restoration of heartbeat in reperfusion. Meanwhile, Sev-CFs-Exo increased conduction velocity (CV), decreased absolute inhomogeneity ($P_{5\text{-}95}$) and inhomogeneity index ($P_{5\text{-}95}/P_{50}$) at T_2 and T_3, as well as promoted the recovery of HR, CV, $P_{5\text{-}95}$ and $P_{5\text{-}95}/P_{50}$ after hypothermic global ischemia-reperfusion injury. Furthermore, Sev-CFs-Exo raised expression and reduced lateralization of Cx43, and improved myocardial infarct sizes and cellular necrosis. However, while cardiac fibroblast-derived exosomes (CFs-Exo) showed similar cardioprotective effects, the outcomes were not as significant.

Conclusion: Sevoflurane reduces the risk of RA and improves ventricular conduction and MIRI by CFs-Exo, and this may be driven by the expression and location of Cx43.

Keywords: anesthetic, extracellular vesicles, arrhythmia, electrophysiology, electrical mapping, connexin 43, Cx43

Introduction

Hypothermia and hyperkalemia protect the myocardium during cardiopulmonary bypass (CPB), however, both are not able to completely alleviate myocardial ischemia-reperfusion injury (MIRI).[1,2] Reperfusion arrhythmia (RA) is a typical manifestation of MIRI, and often occurs immediately after the aorta is opened, typically lasts between 10–30 minutes, and the frequency of occurrence can be as high as 80%.[3] Ventricular arrhythmia, in turn, is the main indicator of RA, resulting in hemodynamic anomaly which has a negative impact on prognosis.[4] Therefore, it is important to identify measures that can be adopted to reduce the risk of RA. One of the major causes of RA is myocardial conduction disorder

Received: 18 February 2023
Accepted: 6 June 2023
Published: 12 June 2023

brought on by cardiomyocyte decoupling. Conduction velocity (CV) and conduction inhomogeneity are important indicators of myocardial conduction.[5,6] In recent years, multi-electrode array (MEA) mapping has emerged as a key technique in the study of cardiac electrophysiology, which can simultaneously record extracellular electrograms from multiple sites in the epicardium and generate isochronous conduction maps according to the recorded data, to visualize changes in electrical conduction.[7]

In a hypoxic myocardium microenvironment, proximal and long-distance signaling occurs between cardiac fibroblasts (CFs) and cardiomyocytes to regulate MIRI.[8,9] A number of previous studies have focused on the growth factor-mediated paracrine signaling pathway, however, emerging evidence has indicated that exosomes are crucial for long-distance signaling in a hypoxic myocardium microenvironment.[10,11] Exosomes are microvesicles released into surrounding bodily fluids by exocytosis after the multivesicular body and plasma membrane are fused. Exosomes are 30–150 nm in diameter and participate in the transmission of intracellular substances and genetic information, and has potential therapeutic effects on a variety of diseases.[12,13] The release of exosomes is affected by several factors; altering the extracellular environment may modify the contents of exosomes, which may then have an impact on the several biological constituents and information released.[14] CFs are the most abundant (60% to 70% of all heart cells) cardiac cells, are crucial for preserving the heart's proper rhythm and conductivity, and have the capacity to produce and secrete collagen.[15,16] In parallel, cardiac fibroblast-derived exosomes (CFs-Exo) have cardioprotective effects and play an important role in MIRI. A previous study has shown that CFs-Exo protects cardiomyocytes against MIRI by suppressing cardiomyocyte pyroptosis through the transport of microRNA-133a.[17] In addition, fibroblast-derived microRNA-423-3p acts as a crucial paracrine mediator of CFs cardioprotection.[18]

Gap junction is a critical channel for cell-to-cell communication to enable the spread of electrical signals in an orderly manner in the heart. Connexins serve as the building blocks for the gap junction.[19] The principal connexin in the ventricle is connexin 43 (Cx43), and its expression is regulated by microRNA-1.[20] Abnormal expression and location of Cx43 in ischemia-reperfusion myocardium is closely related to RA, and up-regulation of Cx43 expression can reduce the risk of RA.[21] Sevoflurane is one of the most commonly utilized halogenated inhalational anesthetics in CPB surgery because of its low blood-gas partition coefficient, high anesthetic efficiency and no discernible influence on heart rates (HR).[22,23] Our previous research found that sevoflurane produced an antiarrhythmic effect by regulating the expression and location of Cx43 in the ventricle which improved electrophysiological stability after ischemia-reperfusion.[24,25] Moreover, cardiac fibroblasts culture medium containing sevoflurane increased the relative expression of Cx43 and enhanced cardiomyocyte activity following hypoxia/reoxygenation, but whether this is driven by exosomes is currently unknown.[26] Therefore, in this study, we hypothesized that sevoflurane would stabilize cardiac conduction and reduce the risk of RA by CFs-Exo.

Materials and Methods

Animals and Treatment

Specific pathogen-free (SPF) grade healthy male SD rats weighing 280–320 g (supplied by the Animal Experimental Center of Guizhou Medical University) were housed at 25 °C with 12 hours of light per day and access to unlimited feed and water. The Animal Experimental Committee of Guizhou Medical University approved the proposed activities (No. 2101051), and the animal disposal process followed the Guide for the Care and Use of Laboratory Animals provided by the National Institutes of Health.

SD rats were randomly divided into four groups (n = 8): the control group (group C), the ischemia-reperfusion group (group IR), the CFs-Exo+group IR (group N+IR), and the exosomes derived from sevoflurane-treated cardiac fibroblasts (Sev-CFs-Exo)+group IR (group S+IR). We injected saline (1.0 mL) in group C and group IR, 200 μg (in a total volume of 1.0 mL) of CFs-Exo and Sev-CFs-Exo in group N+IR and group S+IR respectively through the caudal vein.[17] After 48 hours, hearts were harvested to prepare the Langendorff models.[27] The hearts of group C were balanced perfusion with Krebs–Henseleit (K-H) solution (containing NaCl 120 mM, KCl 4.5 mM, $CaCl_2$ 1.25 mM, $MgCl_26H_2O$ 1.2 mM, KH_2PO_4 1.2 mM, $NaHCO_3$ 20 mM, $C_6H_{12}O_6$ 10 mM; pH = 7.4) for 110 minutes. The hearts of group IR, group N+IR, and group S+IR were balanced perfusion for 20 minutes, followed by inducing cardiac arrest for 60 minutes by suffusing

with St. Thomas's solution (containing NaCl 120 mM, KCl 16 mM, $MgCl_2$ 16.6 mM, $CaCl_2$ 1.2 mM, $NaHCO_3$ 10 mM; pH = 7.8) (4 °C, 20 mL/kg; 10 mL/kg reperfusion after 30 minutes of ischemia), and finally reperfusion with K-H solution for 30 minutes.

Isolation, Identification, and Treatment of CFs

The ventricles of neonatal SD rats were cut, washed with phosphate-buffered solution (PBS) and Penicillin/Streptomycin (PS, Procell Life Science & Technology Co., Ltd., China), and minced. The minced tissue was then softened with an appropriate amount of 0.125% trypsin (Gibco Inc., USA) for 8–10 hours at 4 °C. The tissue was further digested with 0.08% trypsin for 5 minutes in an incubator at 37 °C with 5% CO_2. Digestion was terminated with an equal volume of Dulbecco's Modified Eagle Medium (DMEM, Gibco Inc., USA) containing 10% Fetal Bovine Serum (FBS, Gibco Inc., USA) and 1% PS. These steps were repeated until no visible tissue mass remained. The cell fluid was filtered through a filter (200-mesh), centrifuged at 1000 g for 5 minutes and the resulting pellet was re-suspended with DMEM containing 10% FBS and 1% PS. The cells were cultured in an incubator at 37 °C with 5% CO_2 for 90 minutes, after which the medium was replaced with fresh DMEM containing 10% FBS and 1% PS, then incubation was continued.

Growth and morphological changes were observed with an inverted microscope (Olympus Corporation, Japan) at 40X and 100X magnification at 0H (immediately after differential adhesion for 90 minutes), 24H, 48H, and 72H. Immunofluorescence: CFs from passage 2 (P2) were fixed with 4% paraformaldehyde (PFA, Beijing Soleibao Technology Co., Ltd., China) for 20 minutes, washed thrice with PBS, permeabilized with 0.1% Triton-100 (Beijing Soleibao Technology Co., Ltd., China) for 8 minutes, sealed with 5% bovine serum albumin (BSA, Beijing Soleibao Technology Co., Ltd., China) for 60 minutes at ambient temperature, incubated with vimentin antibody (mouse monoclonal, 1:1000, Proteintech Group, China) for 12 hours at 4 °C, washed thrice with PBS, incubated with fluorescein isothiocyanate (FITC, 1:100, Beijing Soleibao Technology Co., Ltd., China) for 60 minutes and DAPI (Beijing Soleibao Technology Co., Ltd., China) for 10 minutes, then sealed with mounting medium and observed under a confocal laser-scanning microscope (CLSM, Olympus Corporation, Japan).

P2-P3 CFs with 60–70% confluency were randomly divided into the normal group (group N) and the sevoflurane-treated group (group S) according to a completely randomized digital table. For group N, the supernatant was replaced with DMEM containing 10% exosome-depleted fetal bovine serum (Shanghai XP Biomed Ltd, China) and 1% PS. After a similar medium change for group S, the culture bottle was connected to the Vapor2000 (a volatilization pot of anesthetic gas), infusing the cells with 2.5% sevoflurane for an hour. After that, the CFs were cultured for a further 24–48 hours.[28] When the cell confluency reached 80%-95%, the supernatant was collected to extract exosomes.

Enrichment and Identification of Exosomes

Exosomes were enriched using the Exosome Isolation Kit (Umibio Science and Technology Group, China) containing Exosome Concentration Solution (ECS) and Exosomes Purification Filter (EPF). Cell supernatant that had been obtained repeatedly was transferred to a centrifugal tube and centrifuged at 3000 g for 10 minutes at 4 °C to remove the fragment, then added the ECS to react for 20–22 hours at 4 °C. The miscible liquid was centrifuged at 10,000 g for 60 minutes at 4 °C. Exosomes were resuspended with PBS, transferred to a centrifuge tube and centrifuged at 12,000 g for 2 minutes at 4 °C. The supernatant was transferred into the upper chamber of an EPF and centrifuged at 3000 g for 10 minutes at 4 °C. The purified exosomes were collected, determined concentration by protein quantitative analysis, packed in 50–100 μL aliquots, and stored at −80 °C for subsequent experiments.

Transmission electron microscopy (TEM): We added exosomes (10 μL) and uranyl acetate (10 μL) to the copper net for 1 minute and adsorbed the excess liquid with filter paper. Exosomes were analyzed and photographed using a TEM (Hitachi Limited, Japan). Nanoparticle tracking analysis (NTA): The flow nano analyzer (Xiamen Fuliu Biotechnology Co. Ltd, China) was used to test exosomes that had been dissolved and diluted 20 fold. After sample detection was completed, the particle size and concentration information of exosomes had been maintained.

Establishment of the Hypothermic Global Ischemia–Reperfusion Model in SD Rats

SD rats were injected intraperitoneally with 2.5% heparin sodium (3125 IU/Kg) and 1% pentobarbital (60mg/Kg). Once the rat was fully anesthetized and laid flat on the surgical table, the abdomen and mediastinum under the xiphoid process were cut open followed by the thoracic cavity. The heart was immediately dissected with ophthalmic scissors and deposited into a cold K-H solution. The aortic root was thoroughly trimmed and attached to a Langendorff perfusion system. We gradually increased the K- H solution (balanced with 95% O_2 and 5% CO_2) flow velocity to 8–9 mL/minute. The isolated rat heart was retrogradely perfused with constant temperature (37°C). The model was successful if the heart returned to a regular rhythm within 2 minutes and HR was more than 180 beats per minute (bpm).

Observation of HR, RA, and the Time for Restoration of Heartbeat

The HR was determined at the start of monitoring (T_0), after balanced perfusion for 20 minutes (T_1), reperfusion for 15 minutes (T_2), and reperfusion for 30 minutes (T_3). The types, frequencies, and durations of RA were monitored during T_3 and scored based on the Lambeth conventions.[29] We monitored and recorded the time for restoration of a heartbeat after the balanced perfusion and reperfusion of the isolated hearts.

Measurement of CV and Inhomogeneity

The 64-channel MEA mapping system (EMS64-USB-1003, MappingLab Ltd., UK) (8×8, grid; contact material: silver; mesh size: 3.0mm × 3.0mm; electrode diameter: 0.1mm; electrode spacing: 0.43mm; electrode impedance: 1.5–1.7 Ω) was used to collect data at T_1, T_2 and T_3. The 64 electrodes served as positive inputs while aortic intubation represented negative inputs. A positive waveform was recorded when a wavefront was transmitted to the electrode from elsewhere while a negative waveform was recorded at T_1-T_3. The electrode was attached to the surface of the left ventricle (determined by the anatomical marks of the left anterior descending artery, aorta, and atrium) to monitor the cardiac electrical conduction data captured by the EMapRecord 5.0 software (MappingLab Ltd., UK), which was then analyzed with the EmapScope 5.0 software (MappingLab Ltd., UK). Isochrones were drawn from these recordings using the built-in function of the program, and CV over five cardiac cycles across 64 channels was calculated. P_5, P_{50}, and P_{95} data were obtained based on the histograms of the local maximum phase differences. The absolute inhomogeneity ($P_{5\text{-}95}$) and the inhomogeneity index ($P_{5\text{-}95}/P_{50}$) of conduction were calculated with $P_{5–95}$ and $P_{5–95}/P_{50}$ normalized to 1 mm.

Western Blot

The bicinchoninic acid (BCA) kit was used to quantify the proteins of ventricular tissue after perfusion which were then denatured for 8 minutes at 100 °C. Proteins (36 μg) were electrophoresed on 10% SDS-PAGE gels (80V, 25 minutes; 120V, 55 minutes) and the semi-dry electrophoretic transfer system (American Bio-rad Company; 25V, 1mA, 30 minutes) was used to transfer proteins onto polyvinylidene fluoride (PVDF) membranes. After washing with TBS-Tween (TBST, 3×10 minutes for each wash) and blocking with 5% skim milk at room temperature for an hour, the membranes were incubated with primary antibodies (anti-Cx43, 1:5000, rabbit polyclonal, Cell Signaling Technology Inc., USA; anti-GAPDH, 1:5000, rabbit monoclonal, Beijing Boaosen Biotechnology Co., Ltd. Beijing, China) overnight at 4 °C. After washing with TBST (3 x 10 minutes), the membranes were further immunoblotted with secondary antibodies (1:8000, Beijing Soleibao Technology Co., Ltd., China) for an hour at room temperature. Chemiluminescence signals were detected using the enhanced chemiluminescent reagents (ECL, New Cell & Molecular Biotech Co., Ltd., China) and exposed to the automatic gel imaging analysis system (ZF-158, American Bio-rad Company).

Immunofluorescence

In brief, the paraffin sections were dewaxed, hydrated, repaired by the citrate antigen retrieval solution (Beijing Soleibao Technology Co., Ltd., China), washed thrice with PBS, sealed with 5% BSA for 30 minutes, incubated with Cx43 antibody (1:2000, rabbit polyclonal, Cell Signaling Technology Inc., USA) for 8 hours at 4°C, washed thrice with PBS, incubated with FITC (1:100, Beijing Soleibao Technology Co., Ltd., China) for 60 minutes, washed thrice

with PBS, incubated with DAPI (Beijing Soleibao Technology Co., Ltd., China) for 5 minutes, washed thrice with PBS, then sealed with mounting medium and observed under a confocal laser-scanning microscope (CLSM, Olympus Corporation, Japan).

2, 3, 5 – Triphenyl Tetrazolium Chloride (TTC) Staining

At the end of perfusion, three hearts in each group were randomly selected and cut evenly into five pieces along the short axis of the left ventricle. The slices were placed in 1% TTC solution (Beijing Soleibao Technology Co., Ltd., China) for 30 minutes at 37 °C, then fixed with 4% PFA. The infarcted areas (white) and non-infarcted areas (brick red) were recorded by a digital camera, and the infarcted areas were quantified with the ImageJ software.

Hematoxylin-Eosin (HE) Staining

In short, after perfusion, the left ventricular tissues were fixed (4% PFA), dehydrated (graded alcohols), cleared (xylene), paraffin-infiltrated and embedded, in sequence. The microtome (Leica RM2235, Leica microscopic system Shanghai Co., Ltd., China) was used to slice the tissues. The sections were dewaxed (xylene), hydrated (alcohol), stained with hematoxylin (5 minutes), differentiated with 1% hydrochloric acid alcohol (2 seconds), stained with eosin (8 minutes), dehydrated with alcohol and cleared in xylene. Finally, the mounted slides were photographed using a digital slice scanner (Olympus VS200, Olympus Corporation, Japan).

Statistical Analysis

The data were analyzed using the SPSS 18.0 software (SPSS Inc, Chicago, IL, USA). Analysis of Variance (ANOVA) was applied for inter-group and intra-group comparison, and GraphPad Prism 8.0 software was used to prepare the Figures. Values are presented as the mean ± standard deviation (SD). $P<0.05$ was considered statistically significant. The P values are indicated in the Figures by the following symbols: * or #, $P<0.05$, ** or ##, $P<0.01$, and *** or ###, $P<0.001$ respectively. T_0, the moment of monitoring; T_1, balanced perfusion for 20 minutes; T_2, reperfusion for 15 minutes; T_3, reperfusion for 30 minutes.

Results

Identification of Primary CFs, and Comparison of CFs-Exo and Sev-CFs-Exo

Under the inverted microscope, some of the cells were observed to adhere to the bottom almost immediately after differential adhesion and presented with round or oval-shaped cells. The non-adherent cells were represented by the spherical bright areas and presented at low cell confluency (Figure 1A). After twenty-four hours, the cells protruded pseudopodia with long spindle, triangle, and polygon shapes, accompanied by an increase in adherent cells and cell confluency (Figure 1A). On the second day, the cell morphologies were varied, the outlines were clear, the nucleus and nucleolus were clearly visible, all the cells had adhered to the bottom, and the cell confluency was more than 85% (Figure 1A). On the third day, the cells showed long spindle-shaped, irregular polygons, containing 1–3 nuclei, closely arranged, and the confluency was more than 95% (Figure 1A). Trypan blue staining indicated more than 90% cell survival for the isolated CFs. Immunofluorescence showed that over 98% of the CFs were positive for vimentin (Figure 1B). In conclusion, these results indicated that the survival rate and purity of primary CFs met the experimental requirements.

TEM revealed that exosomes of the two groups were biconcave discs and either round or oval in shape (Figure 2A and D). NTA showed that Group C and Group S had average particle sizes of 73.80 nm and 70.51 nm (Figure 2B and E), and concentrations of 6.25E+9 particles/mL and 6.76E+9 particles/mL, respectively (Figure 2C and F). These outcomes confirmed that exosomes were successfully enriched and there was little difference between the two groups.

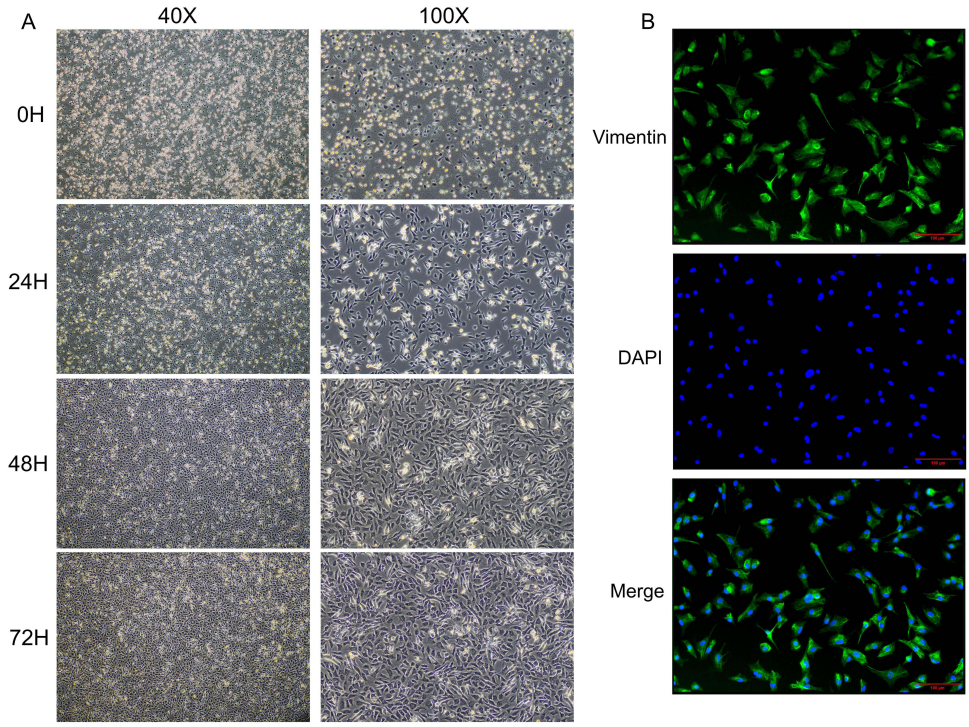

Figure 1 Identification of primary cardiac fibroblasts. (**A**) The morphology and confluency of cardiac fibroblasts at each point (0H, 24H, 48H, 72H are the time after differential adhesion). (**B**) The purity of cardiac fibroblasts identified by immunofluorescence.

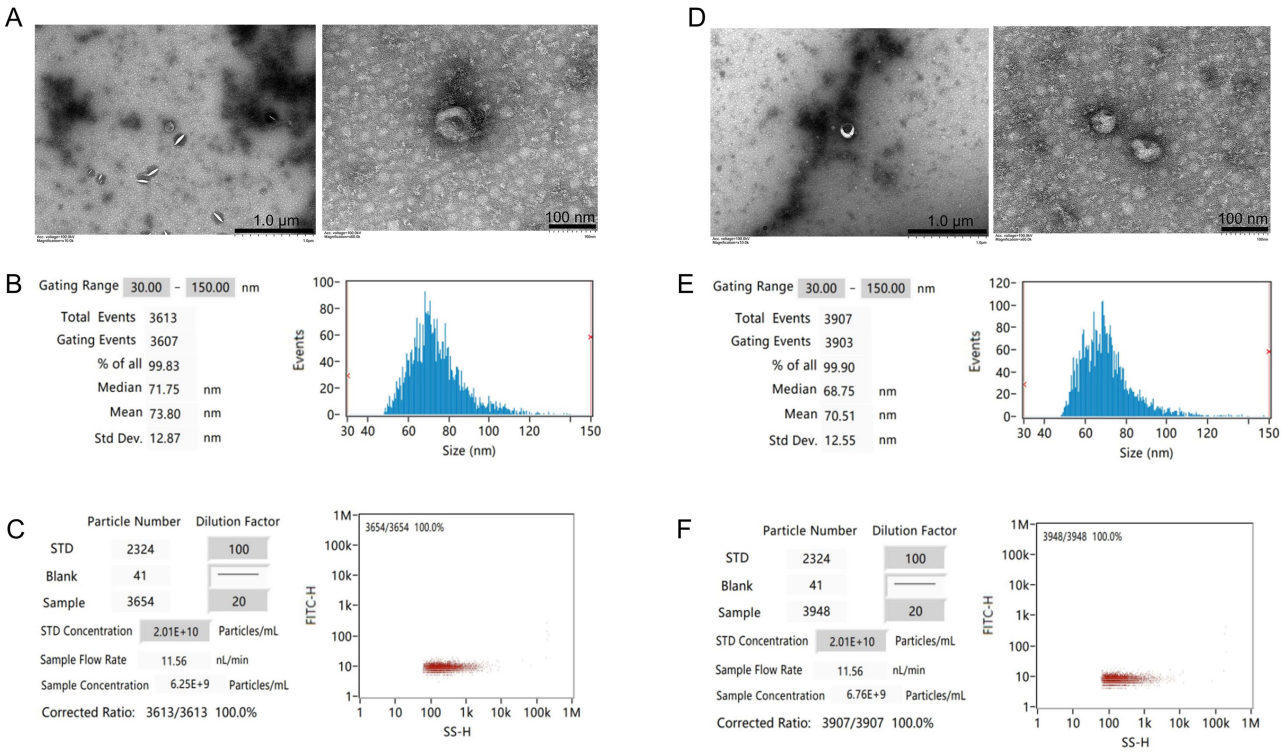

Figure 2 Identification and comparison of exosomes. The morphology (**A** and **D**), diameters distribution (**B** and **E**), and concentration (**C** and **F**) of the CFs-Exo and Sev-CFs-Exo were observed by the transmission electron microscope and nanoparticle tracking analysis (The former is CFs-Exo).

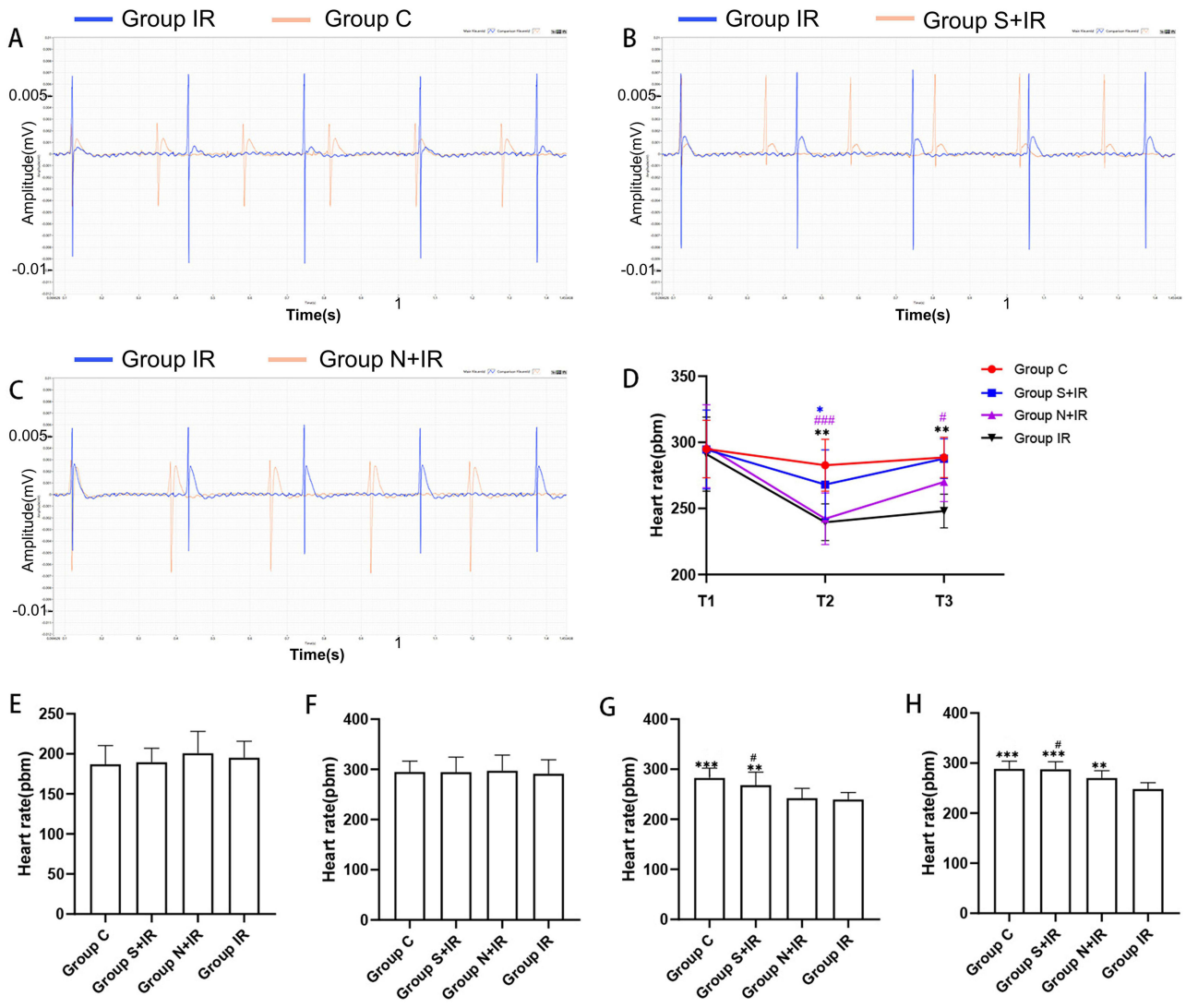

Figure 3 Effects of CFs-Exo and Sev-CFs-Exo on heart rates. Representative biphasic electrograms from a single channel were obtained from isolated hearts in the control condition (**A**) and the presence of Sev-CFs-Exo (**B**) and CFs-Exo (**C**). The heart rates in the four groups: reperfusion vs balanced perfusion (**D**), *group IR, #(purple) group N+IR, *(blue) group S+IR. Comparison of heart rates in the four groups at T_0 (**E**), T_1 (**F**), T_2 (**G**), and T_3 (**H**),*vs group IR, #vs group N+IR. Data from n = 8 hearts. **P<0.01, *** or ###P<0.001.

Effects of CFs-Exo and Sev-CFs-Exo on HR and RA After Hypothermic Global Ischemia-Reperfusion

Enlarged traces from a single channel were shown in Figures 3A–C. When compared to T_1, HR was significantly slower at T_2 and T_3 in group N+IR and group IR, at T_2 in group S+IR, and there was no significant difference at T_3 for group S+IR and at T_2 and T_3 for group C (Figure 3D). There was no significant difference in HR among the four groups at T_0 and T_1 (Figure 3E and F). When compared to group IR, HR considerably increased at T_2 and T_3 in group C and group S+IR, and at T_3 in group N+IR, but there was no significant difference at T_2 in group N+IR. The HR at T_2 and T_3 in group S+IR was significantly higher than in group N+IR (Figure 3G and H).

Representative arrhythmias acquired by MEA were shown in Figure 4A. Compared with group IR, the score and duration of RA in group N+IR and group S+IR were significantly lower. The duration of RA in group S+IR was substantially shorter compared with group N+IR, however, there was no significant difference in RA score between the two groups (Figure 4B and 4C). There was no noticeable difference in the time for restoration of heartbeats among the four groups during balanced perfusion

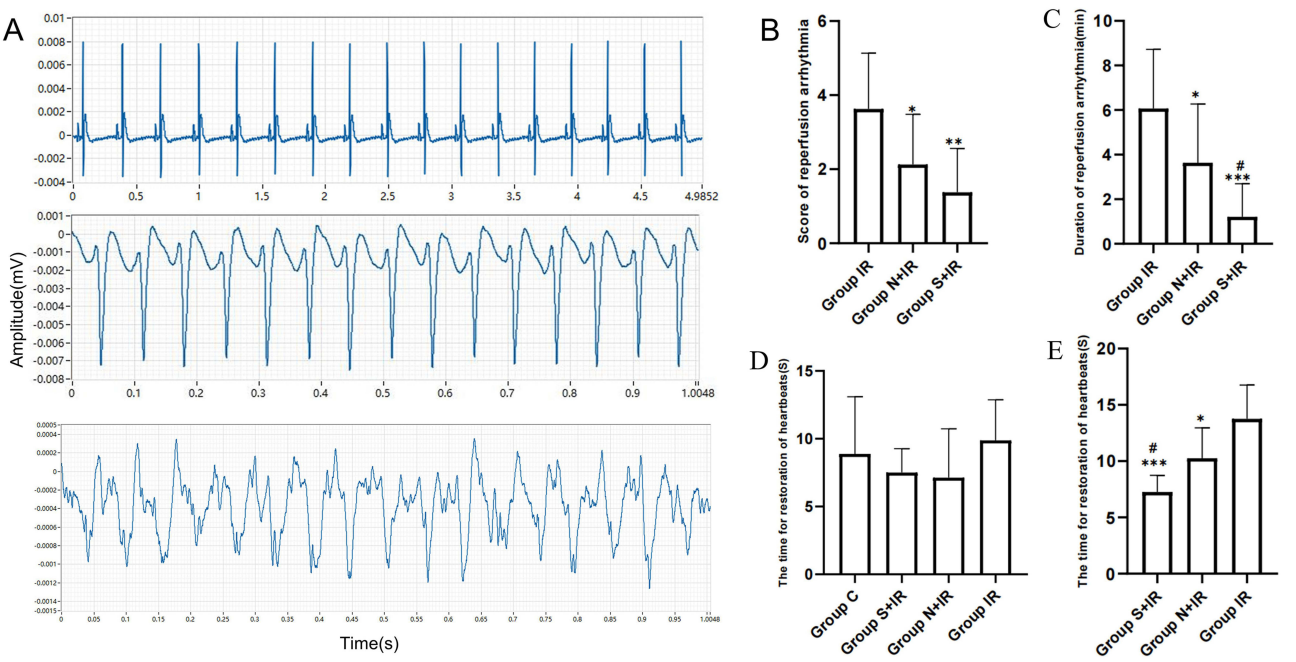

Figure 4 Effects of CFs-Exo and Sev-CFs-Exo on reperfusion arrhythmia. (**A**) Typical electrograms were obtained from spontaneously beating hearts during reperfusion for 30 minutes: normal electrocardiogram (top), ventricular tachycardia (middle) and ventricular fibrillation (bottom). The score basing on the Lambeth conventions (**B**) and duration (**C**) of reperfusion arrhythmia. The time for restoration of heartbeats at the point of balanced perfusion (**D**) and reperfusion (**E**). *vs group IR, #vs group N+IR. Data from n = 8 hearts. **P<0.01, ***P<0.001.

(Figure 4D). The time for restoration of heartbeats during reperfusion in group S+IR and group N+IR was significantly shorter than that in group IR, and significantly shorter in group S+IR compared with group N+IR (Figure 4E).

Effects of CFs-Exo and Sev-CFs-Exo on Ventricular CV After Hypothermic Global Ischemia-Reperfusion

Figure 5A displayed the typical activation maps at T_2, while Supplementary Figure 1 showed the maps at T_1 and T_3. There was no significantly altered CV among the four groups at T_1 (Figure 5B). At T_2 and T_3, CV was significantly increased in group C, group S+IR and group N+IR compared with group IR, while the CV in group S+IR was higher than in group N+IR (Figure 5C and D). Compared with T_1, CV considerably decreased at T_2 and T_3 in group N+IR and group IR, as well as at T_2 in group S+IR, however, there was no significant change at T_3 for group S+IR and at T_2 and T_3 for group C (Figure 5E).

Effects of CFs-Exo and Sev-CFs-Exo on Ventricular Conduction Inhomogeneity After Hypothermic Global Ischemia-Reperfusion

The typical isochrone maps at T_2 were shown in Figure 6A, and the maps at T_1 and T_3 were shown in Supplementary Figure 2. $P_{5\text{-}95}$ and $P_{5\text{-}95}/P_{50}$ among the four groups at T_1 did not differ significantly (Figure 6B and E). At T_2 and T_3, $P_{5\text{-}95}$ and $P_{5\text{-}95}/P_{50}$ were significantly decreased in group C, group S+IR and group N+IR compared to group IR, while that in group S+IR was significantly lower than in group N+IR (Figure 6C, D, F and G). Compared with T_1, $P_{5\text{-}95}$ and $P_{5\text{-}95}/P_{50}$ were noticeably increased at T_2 and T_3 in group N+IR and group IR, as well as at T_2 in group S+IR, however, there was no significant change at T_3 in group S+IR and at T_2 and T_3 in group C (Figure 6H and I).

Effects of CFs-Exo and Sev-CFs-Exo on Cx43 and MIRI

The protein quantitative analysis revealed that the expression of Cx43 in group C and group S+IR was significantly higher than that in group IR, while group S+IR and group IR did not differ much from group N+IR (Figure 7A). Immunofluorescence showed that a mass of Cx43 was distributed on the lateral membrane in group IR. The redistribution

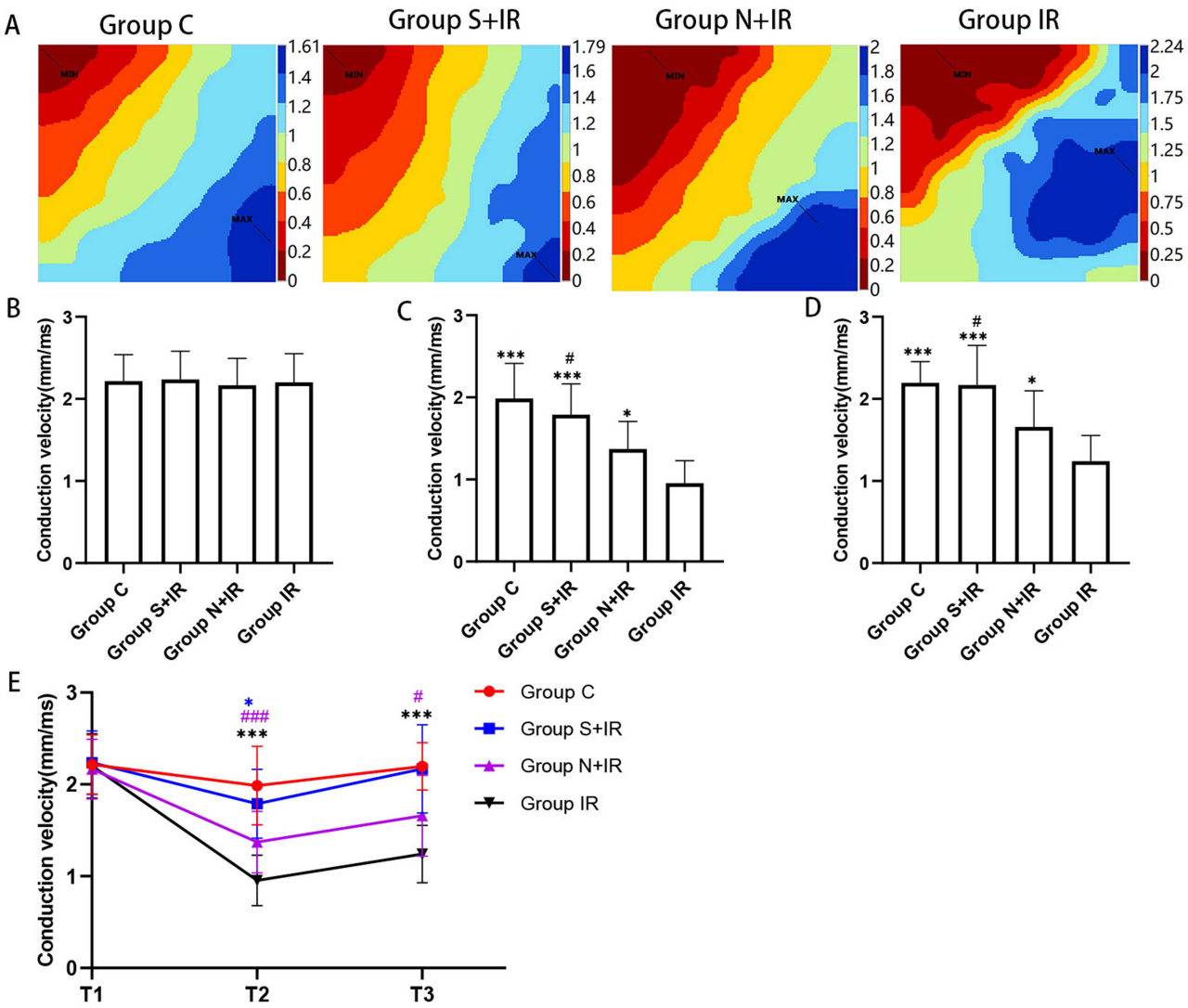

Figure 5 Effects of CFs-Exo and Sev-CFs-Exo on conduction velocity. (**A**) Classic activation maps were obtained in the four groups at T_2. The conduction velocity at T_1 (**B**), T_2 (**C**), and T_3 (**D**), *vs group IR, #vs group N+IR. Reperfusion vs balanced perfusion (**E**), *group IR, #(purple) group N+IR, *(blue) group S+IR. MAX and MIN are the maximum and minimum values of local activation time respectively, which is contrary to conduction velocity. Data from n = 8 hearts. *** or ###P<0.001.

to the lateral membrane of Cx43 decreased significantly after treatment of Sev-CFs-Exo or CFs-Exo, while Cx43 in group C was mainly distributed in the intercalated disc and arranged neatly (Figure 7B). The infarct areas in group C, group S+IR, and group N+IR were significantly less than in group IR, with group S+IR significantly lower when compared to group N+IR (Figure 7C). HE staining revealed loose connections between cells, vacuolar changes, pyknosis and uneven cytoplasmic staining in group IR, while similar changes were noted in group N+IR, but to a lesser extent. The cells showed slight swelling and enlarged nuclei, but there were no signs of necrosis in group S+IR. Concurrently, there was no obvious abnormality in group C (Figure 7D).

Discussion

In this study, we investigated the effects of Sev-CFs-Exo and CFs-Exo on RA, ventricular electrical conduction, and reperfusion injury using a hypothermic global ischemia-reperfusion model. MEA monitored the electrical signals from the left ventricular regional areas to produce isochronous maps and measured the conduction temporal and spatial inhomogeneity. The data obtained showed that CFs-Exo lowered the risk of RA, increased ventricular CV, reduced changes in conduction

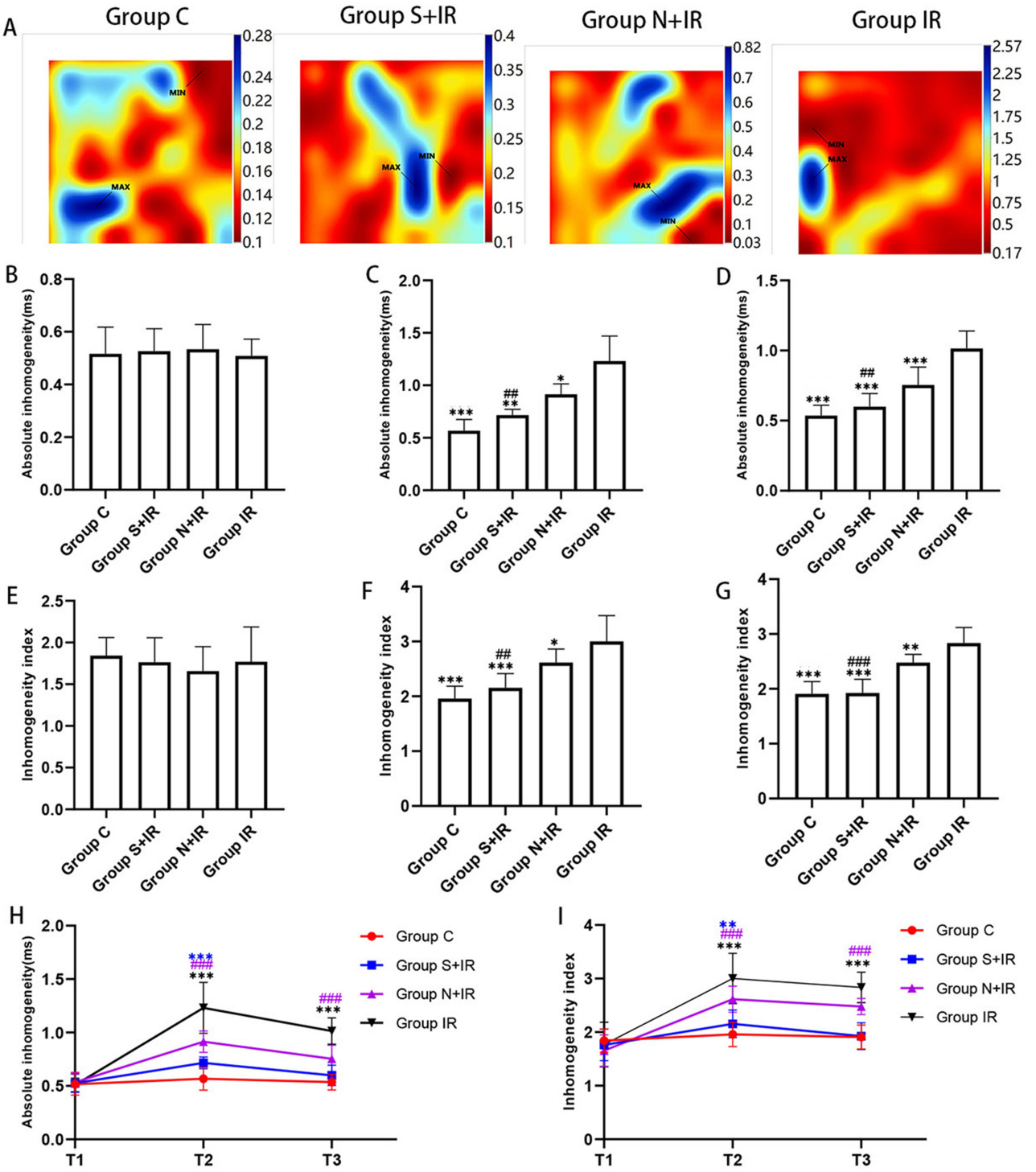

Figure 6 Effects of CFs-Exo and Sev-CFs-Exo on inhomogeneity. (**A**) Representative inhomogeneity maps were acquired in the four groups at T_2. The absolute inhomogeneity and inhomogeneity index respectively at T_1 (**B** and **E**), T_2 (**C** and **F**), and T_3 (**D** and **G**), *vs group IR, #vs group N+IR. Reperfusion vs balanced perfusion (**H** and **I**), *group IR, #(purple) group N+IR, *(blue) group S+IR. MAX and MIN are the maximum and minimum values of inhomogeneity respectively. Data from n = 8 hearts. ** or ##P<0.01, *** or ###P<0.001.

inhomogeneity following reperfusion, and improved MIRI. Sevoflurane exerted cardioprotective outcomes by enhancing the effects of CFs-Exo, which may be related to its regulating the expression and location of Cx43.

When myocardial blood flow is restored after CPB, this could lead to reperfusion injury, which causes cardiac dysfunction such as no-reflow phenomena, myocardial stunning, RA, and other symptoms.[30] The myocardial protection

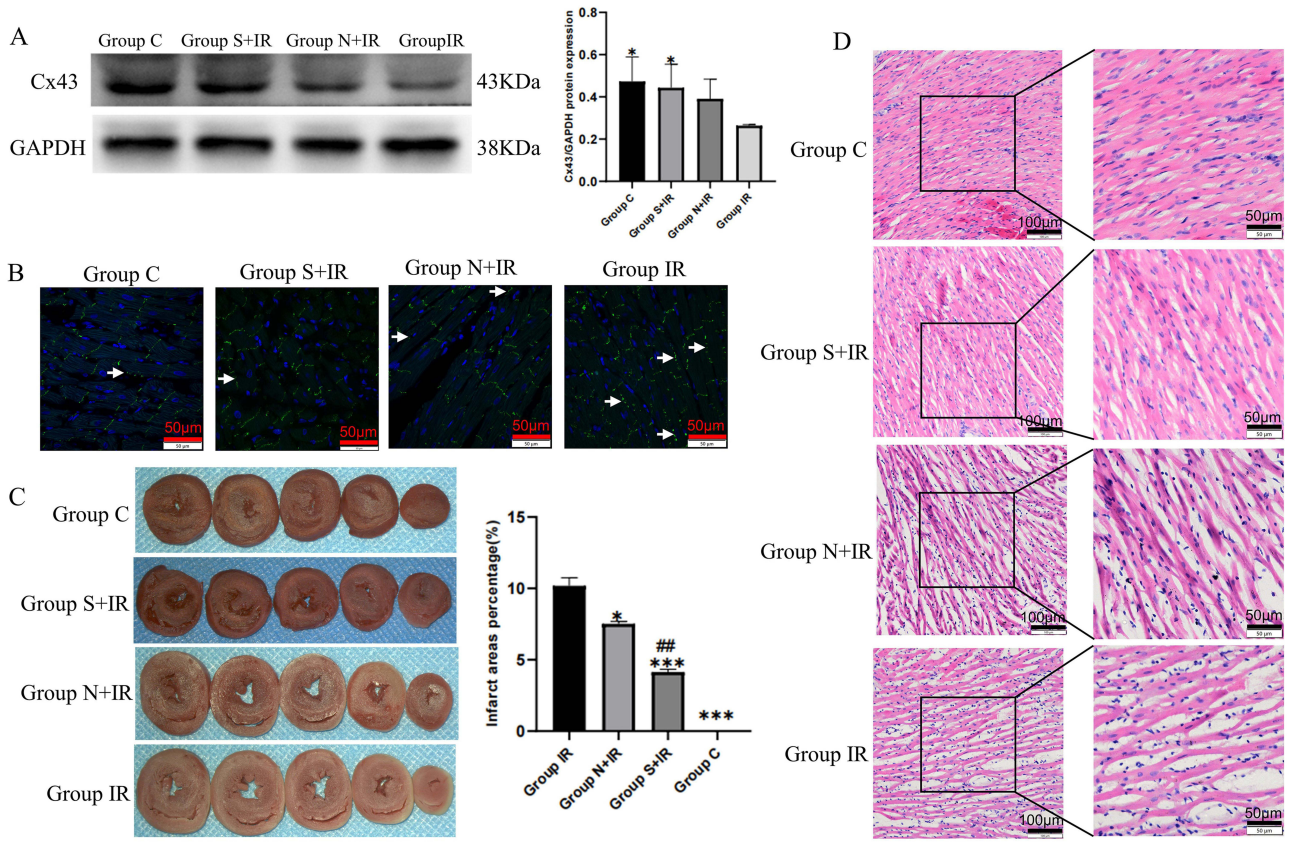

Figure 7 Effects of CFs-Exo and Sev-CFs-Exo on Cx43 and myocardial ischemia-reperfusion injury. (**A** and **B**) The relative expression and location of Cx43 in the four groups assessed by Western blotting assay and immunofluorescence, Cx43 is stained green with FITC, while the nucleus is dyed blue with DAPI, and the lateral Cx43 is as indicated by the arrow. (**C**) 2, 3, 5 – Triphenyl tetrazolium chloride staining determined myocardial infarct size. (**D**) Hematoxylin-Eosin staining evaluated changes in myocardial morphology. *vs group IR, #vs group N+IR. Data from n = 3 hearts. ##P<0.01, ***P<0.001.

strategy during CPB, neurohumoral variables as well as ischemic severity and duration are risk factors for RA.[31,32] In this study, the Langendorff perfusion device was applied to establish a hypothermic global myocardial ischemia-reperfusion model in SD rats. The use of this model enabled the direct impact of Sev-CFs-Exo on the heart to be assessed objectively by excluding neurohumoral activation and other parameters.

MEA offers higher stability and reproducibility and does not mechanically harm the epicardial surface when used to monitor the CV and dispersion of isolated hearts as opposed to employing custom-made electrodes and monophasic action potential. Simultaneously, the electrical activity of the cardiomyocytes at the electrode contact site may be more accurately recorded, and at the same time, the temporal and spatial inhomogeneity in conduction can be more accurately assessed.[33] Theoretically, the conduction inhomogeneity can be either a primary or secondary abnormality caused by slow CV. Furthermore, the conduction inhomogeneity index can be employed to differentiate between both types of abnormalities.[34] The findings of this study show that the absolute inhomogeneity and conduction inhomogeneity index change synchronously, demonstrating that the change in inhomogeneity after hypothermic global ischemia-reperfusion is primary. A study has observed that the rat hearts resumed sinus rhythm and conduction within 10 to 15 minutes after 60 minutes of arrests at room temperature.[35] However, the outcomes of this study do not concur with those and may be due to the fact that different preventive measures were used during cardiac arrest as the electrical conduction of the SD rat hearts had not recovered within 30 minutes of reperfusion. The experimental results also revealed that while HR, CV, and conduction heterogeneity during the 30 minutes of reperfusion did not recover after CFs-Exo treatment, recovery was noted following Sev-CFs-Exo treatment, implying that sevoflurane can promote the recovery of cardiac conduction after reperfusion by CFs-Exo.

Both animal and human clinical trials have demonstrated that sevoflurane has cardioprotective benefits.[36,37] However, major investigations on the cardioprotective effects of sevoflurane have focused on cardiomyocytes. The heart is made up of many other types of cells such as CFs, smooth muscle cells, and endothelial cells, but limited research has been undertaken with these other cells.[38] CFs perform a crucial paracrine function and contribute significantly to the emergence of RA.[16] Vimentin is the most sensitive marker of CFs.[16] Numerous investigations have shown that CFs-Exo has cardioprotective functions.[17,18,39] Primary CFs were extracted from the ventricles of neonatal SD rats and authenticated by morphology and vimentin. Afterward, exosomes were isolated from the fibroblast-conditioned medium and identified using TEM and NTA prior to investigating how exosomes function in the paracrine cardioprotection of CFs. Once the exosomes had been confirmed and the CFs-Exo were transplanted into SD rats, the hearts were removed to prepare the ischemia-reperfusion model. Our demonstration that CFs-Exo can improve MIRI is in agreement with previously published research.[17,39] Furthermore, this study also showed that CFs-Exo can enhance ventricular electrical conductivity and lower the risk of RA following hypothermic ischemia-reperfusion.

To determine if sevoflurane can reduce the occurrence of RA through CFs-Exo, we mixed sevoflurane with CFs to obtain Sev-CFs-Exo. Initially, the study revealed that while the effects varied between the two groups of exomes, there were little changes in shape, particle size, and concentration of exosomes, which established that altering the external CFs environment led to a change in the composition of CFs-Exo. This concurs with the finding that contended that ischemia post-conditioning can boost the cardioprotective effects of CFs-Exo.[18] Secondly, the cardioprotective effects of Sev-CFs-Exo and CFs-Exo were compared in the hypothermic ischemia-reperfusion model, and while both had similar benefits, the former was more pronounced. Taken together, we have demonstrated that sevoflurane is cardioprotective by enhancing the role of CFs-Exo.

Based on the amino acid sequence of the carboxyl-terminal domain, connexins are classified into various subtypes. Cx43 is the largest subtype in the ventricle and changes in Cx43 expression are crucial in RA.[9,21] A previous study showed that the expression of miR-1 increased and was subsequently regulated to lower the expression of Cx43 under oxidative stress.[20] Our investigation demonstrated that while CFs-exo boosted the expression of Cx43 in ventricular tissues, however, Sev-CFs-Exo significantly enhanced it. Meanwhile, both of them could reduce the distribution of Cx43 to the lateral membrane. Therefore, we speculate that Sev-CFs-Exo improves ventricular conduction and lowers the risk of RA by regulating the expression and location of Cx43.

The current study has certain limitations. Firstly, while we demonstrated only minor differences in terms of cell morphology, size, and density between Sev-CFs-Exo and CFs-Exo, no further analysis was conducted on the changes noted in proteins. Secondly, we did not extend the study to understand the precise mechanism(s) used by Sev-CFs-Exo to improve ventricular conduction and reduce the risk of RA, but this will be undertaken in our future research.

Conclusion

In summary, CFs-Exo can reduce the risk of RA and improve ventricular conduction and MIRI. Furthermore, sevoflurane plays an important cardioprotective function by enhancing the effects of CFs-Exo.

Acknowledgments

The authors would like to express their gratitude to EditSprings for the expert linguistic services provided.

Disclosure

The authors report no conflicts of interest in this work.

References

1. De Hert S, Moerman A. Myocardial injury and protection related to cardiopulmonary bypass. *Best Pract Res Clin Anaesthesiol*. 2015;29(2):137–149. doi:10.1016/j.bpa.2015.03.002
2. Tang J, Gao H, Liu Y, et al. Network construction of aberrantly expressed miRNAs and their target mRNAs in ventricular myocardium with ischemia-reperfusion arrhythmias. *J Cardiothorac Surg*. 2020;15(1):216. doi:10.1186/s13019-020-01262-4
3. Kadric N, Osmanovic E. Rhythm disturbance after myocardial revascularization. *Med Arch*. 2017;71(6):400–403. doi:10.5455/medarh.2017.71.400-403
4. Lan YT, Lee JC, Wetzel G. Postoperative arrhythmia. *Curr Opin Cardiol*. 2003;18(2):73–78. doi:10.1097/00001573-200303000-00001

5. Hernández-Romero I, Guillem MS, Figuera C, et al. Optical imaging of voltage and calcium in isolated hearts: linking spatiotemporal heterogeneities and ventricular fibrillation initiation. *PLoS One*. 2019;14(5):e0215951. doi:10.1371/journal.pone.0215951
6. Han B, Trew ML, Zgierski-Johnston CM. Cardiac conduction velocity, remodeling and arrhythmogenesis. *Cells*. 2021;10(11):2923. doi:10.3390/cells10112923
7. Wu Q, Liu H, Liao J, et al. Colchicine prevents atrial fibrillation promotion by inhibiting IL-1β-induced IL-6 release and atrial fibrosis in the rat sterile pericarditis model. *Biomed Pharmacother*. 2020;129:110384. doi:10.1016/j.biopha.2020.110384
8. Pellman J, Zhang J, Sheikh F. Myocyte-fibroblast communication in cardiac fibrosis and arrhythmias: mechanisms and model systems. *J Mol Cell Cardiol*. 2016;94:22–31. doi:10.1016/j.yjmcc.2016.03.005
9. Jin Y, Zhou T, Feng Q, et al. Inhibition of MicroRNA-206 ameliorates ischemia-reperfusion arrhythmia in a mouse model by targeting connexin43. *J Cardiovasc Transl Res*. 2020;13(4):584–592. doi:10.1007/s12265-019-09940-y
10. Flores-Vergara R, Olmedo I, Aránguiz P, et al. Communication between cardiomyocytes and fibroblasts during cardiac ischemia/reperfusion and remodeling: roles of tgf-β, ctgf, the renin-angiotensin axis, and non-coding RNA molecules. *Front Physiol*. 2021;12:716721. doi:10.3389/fphys.2021.716721
11. Chen P, Wang L, Fan X, et al. Targeted delivery of extracellular vesicles in heart injury. *Theranostics*. 2021;11(5):2263–2277. doi:10.7150/thno.51571
12. Kalluri R, LeBleu VS. The biology, function, and biomedical applications of exosomes. *Science*. 2020;367(6478):eaau6977. doi:10.1126/science.aau6977
13. Pegtel DM, Gould SJ. Exosomes. *Annu Rev Biochem*. 2019;88:487–514. doi:10.1146/annurev-biochem-013118-111902
14. Hessvik NP, Llorente A. Current knowledge on exosome biogenesis and release. *Cell Mol Life Sci*. 2018;75(2):193–208. doi:10.1007/s00018-017-2595-9
15. Tallquist MD, Molkentin JD. Redefining the identity of cardiac fibroblasts. *Nat Rev Cardiol*. 2017;14(8):484–491. doi:10.1038/nrcardio.2017.57
16. Tallquist MD. Developmental pathways of cardiac fibroblasts. *Cold Spring Harb Perspect Biol*. 2020;12(4):a037184. doi:10.1101/cshperspect.a037184
17. Liu N, Xie L, Xiao P, et al. Cardiac fibroblasts secrete exosome microRNA to suppress cardiomyocyte pyroptosis in myocardial ischemia/reperfusion injury. *Mol Cell Biochem*. 2022;477(4):1249–1260. doi:10.1007/s11010-021-04343-7
18. Luo H, Li X, Li T, et al. microRNA-423-3p exosomes derived from cardiac fibroblasts mediates the cardioprotective effects of ischaemic post-conditioning. *Cardiovasc Res*. 2019;115(7):1189–1204. doi:10.1093/cvr/cvy231
19. Rodríguez-Sinovas A, Sánchez JA, Valls-Lacalle L, et al. Connexins in the heart: regulation, function and involvement in cardiac disease. *Int J Mol Sci*. 2021;22(9):4413. doi:10.3390/ijms22094413
20. Wahl CM, Schmidt C, Hecker M, et al. Distress-mediated remodeling of cardiac connexin-43 in a novel cell model for arrhythmogenic heart diseases. *Int J Mol Sci*. 2022;23(17):10174. doi:10.3390/ijms231710174
21. Cheng J, Sun C, Zhang J, et al. The protective effects of preconditioning with dioscin on myocardial ischemia/reperfusion-induced ventricular arrhythmias by increasing connexin 43 expression in rats. *J Cardiovasc Pharmacol Ther*. 2019;24(3):262–268. doi:10.1177/1074248418801567
22. Edgington TL, Muco E, Maani CV. Sevoflurane. In: *StatPearls [Internet]*. Treasure Island (FL): StatPearls Publishing; 2022.
23. Uhlig C, Labus J. Volatile versus intravenous anesthetics in cardiac anesthesia: a narrative review. *Curr Anesthesiol Rep*. 2021;11(3):275–283. doi:10.1007/s40140-021-00466-1
24. Li WC, Gao H, Gao J, et al. Antiarrhythmic effect of sevoflurane as an additive to HTK solution on reperfusion arrhythmias induced by hypothermia and ischemia is associated with the phosphorylation of connexin 43 at serine 368. *BMC Anesthesiol*. 2019;19(1):5. doi:10.1186/s12871-018-0656-8
25. Wang G, Dai D, Gao H, et al. Sevoflurane alleviates reperfusion arrhythmia by ameliorating TDR and MAPD90 in isolated rat hearts after ischemia-reperfusion. *Anesthesiol Res Pract*. 2019;2019:7910930. doi:10.1155/2019/7910930
26. Niu Z, Wang G, Gao H, et al. Effects of hypothermic hypoxia/reoxygenation fibroblast culture medium containing sevoflurane on cardiomyocytes. *Ther Hypothermia Temp Manag*. 2022;12(1):24–29. doi:10.1089/ther.2020.0049
27. Hou Z, Qin X, Hu Y, et al. Longterm exercise-derived exosomal miR-342-5p: a novel exerkine for cardioprotection. *Circ Res*. 2019;124(9):1386–1400. doi:10.1161/CIRCRESAHA.118.314635
28. Xie H, Liu Q, Qiao S, et al. Delayed cardioprotection by sevoflurane preconditioning: a novel mechanism via inhibiting Beclin 1-mediated autophagic cell death in cardiac myocytes exposed to hypoxia/reoxygenation injury. *Int J Clin Exp Pathol*. 2015;8(1):217–226.
29. Curtis MJ, Walker MJ. Quantification of arrhythmias using scoring systems: an examination of seven scores in an in vivo model of regional myocardial ischemia. *Cardiovasc Res*. 1988;22(9):656–665. doi:10.1093/cvr/22.9.656
30. Ashraf T, Khan MN, Afaque SM, et al. Clinical and procedural predictors and short-term survival of the patients with no-reflow phenomenon after primary percutaneous coronary intervention. *Int J Cardiol*. 2019;294:27–31. doi:10.1016/j.ijcard.2019.07.067
31. Manning AS, Hearse DJ. Reperfusion-induced arrhythmias: mechanisms and prevention. *J Mol Cell Cardiol*. 1984;16(6):497–518. doi:10.1016/s0022-2828(84)80638-0
32. Jang YH, Kim JH, Lee YC. Mitochondrial ATP-sensitive potassium channels play a role in reducing both myocardial infarction and reperfusion arrhythmia in remote ischemic preconditioned hearts. *Anesth Pain Med*. 2017;7(1):e42505. doi:10.5812/aapm.42505
33. Kim JS, Choi SW, Park YG, et al. Impact of high-dose irradiation on human iPSC-derived cardiomyocytes using multi-electrode arrays: implications for the antiarrhythmic effects of cardiac radioablation. *Int J Mol Sci*. 2021;23(1):351. doi:10.3390/ijms23010351
34. Dong X, Tse G, Hao G, et al. Heterogeneities in ventricular conduction following treatment with heptanol: a multi-electrode array study in langendorff-perfused mouse hearts. *Life*. 2022;12(7):996. doi:10.3390/life12070996
35. Jabr RI, Braveny P, Juggi JS. Recovery of the conduction system from ischemic arrest and cardioplegia in perfused rat heart. *Can J Cardiol*. 1988;4(2):90–96.
36. Frädorf J, Huhn R, Weber NC, et al. Sevoflurane-induced preconditioning: impact of protocol and aprotinin administration on infarct size and endothelial nitric-oxide synthase phosphorylation in the rat heart in vivo. *Anesthesiology*. 2010;113(6):1289–1298. doi:10.1097/ALN.0b013e3181f97fec
37. De Hert SG, Vander Linden PJ, Cromheecke S, et al. Choice of primary anesthetic regimen can influence intensive care unit length of stay after coronary surgery with cardiopulmonary bypass. *Anesthesiology*. 2004;101(1):9–20. doi:10.1097/00000542-200407000-00005

38. Litviňuková M, Talavera-López C, Maatz H, et al. Cells of the adult human heart. *Nature*. 2020;588(7838):466–472. doi:10.1038/s41586-020-2797-4
39. Abrial M, Da Silva CC, Pillot B, et al. Cardiac fibroblasts protect cardiomyocytes against lethal ischemia-reperfusion injury. *J Mol Cell Cardiol*. 2014;68:56–65. doi:10.1016/j.yjmcc.2014.01.005